NIP-WAVE TOMOGRAPHY FOR CONVERTED WAVES

C. Vanelle and D. Gajewksi

email: *claudia.vanelle@zmaw.de*
keywords: *tomography, CRS, converted waves*

ABSTRACT

In theory, model building techniques developed for PP surveys are equally applicable to obtain shear velocities if SS data are available. In practice, however, if shear waves are acquired at all, they are most often recorded as PS conversions. For these data, PP model-building techniques cannot be applied. We suggest a new method to combine PP and PS data to obtain a shear velocity model. The method is based on the NIP wave tomography and uses wave field attributes determined with common reflection surface stacking of the data in combination with ray tracing.

INTRODUCTION

Ever since the introduction of ocean bottom acquisition converted waves have gained importance in exploration seismics (e.g. Tsvankin, 2001). Excitation of shear waves requires significantly more effort than generation of P waves. It is not only difficult but also costly. Since shear information is also contained in the data of PS converted waves, these have been the focus of shear wave exploration for quite some time now.

There are many advantages of taking shear waves into consideration. For example, the presence of gas clouds leads to high absorption for the P waves and makes imaging under such regions inadequate for PP surveys. Shear waves, on the other hand, do not suffer from the absorption (Stewart et al., 2003). Another example where converted waves are beneficial is imaging of targets with weak PP and strong PS impedance contrasts, e.g., for certain types of shale-sand boundaries (Stewart et al., 2003). Due to the smaller velocity of shear waves they can be used to enhance the seismic resolution. This is particularly interesting for the investigation of steeply-inclined near-surface structures (Stewart et al., 2003). Finally, shear waves are essential for the detection and quantification of seismic anisotropy (e.g. Tsvankin, 2001).

Shear waves are also important for reservoir characterisation because parameters like porosity and permeability have strong influence on shear velocities (e.g. Nelson, 2001). Thus, the determination of shear velocities provides a direct means for the prediction of reservoir parameters. For example, it is possible to obtain information on the density and orientation of fractures from converted waves (e.g. Gaiser and Van Dok, 2003) since these fractures lead to seismic anisotropy.

Despite their advantages, shear waves also exhibit serious disadvantages. As already pointed out, for practical reasons the acquisition is usually restricted to converted waves. However, standard techniques for the processing of PP data cannot always be applied to these data.

In contrast to monotypic (i.e. PP or SS) reflections, the ray paths of converted waves are asymmetric with respect to interchanging sources and receivers. In particular in the presence of lateral inhomogeneities or anisotropy, the move-out of a converted wave becomes asymmetric because it contains a linear term, the so-called diodic move-out (Thomsen, 1999). This prevents the application of NMO correction in CMP gathers, which is based on the assumption of symmetric ray paths.

This problem is closely-related to the conversion point dispersal. Although there is a similar phenomenon for monotypic waves, the reflection point dispersal, that effect has a larger magnitude for converted waves.
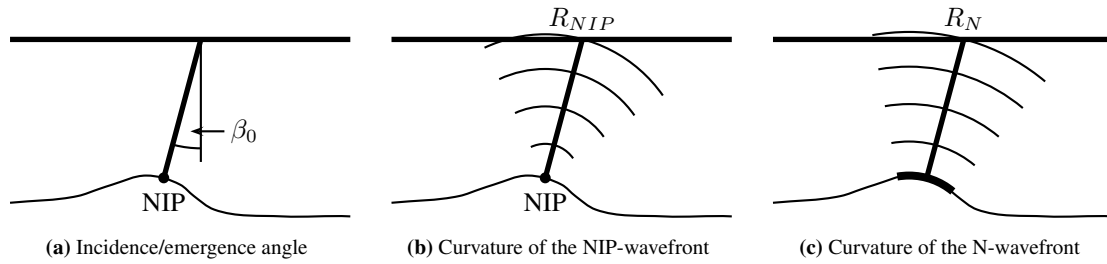
(a) Incidence/emergence angle   (b) Curvature of the NIP-wavefront   (c) Curvature of the N-wavefront

Figure 1: The meaning of the ZO-CRS parameters β_0, K_{NIP}, and K_N. In (b) $K_{NIP} = 1/R_{NIP}$; in (c) $K_N = 1/R_N$.

For these reasons, PS data are sorted in common conversion point (CCP) gathers instead of CMP. Unfortunately, the determination of the CCP itself can be rather complicated (e.g. Tessmer et al., 1990; Thomsen, 1999). Also, it is by no means trivial to obtain a velocity model from the subsequent processing. For example, neglecting the sign of the offset during the CCP binning can lead to a bimodal velocity spectrum due to the diodic move-out (Thomsen, 1999).

Migration-based velocity model-building techniques (e.g. Al-Yahya, 1989) can be used for converted waves. In these methods, residual move-out in the CRP gathers is evaluated for a model update. However, one has to be cautious: due to the asymmetric ray paths in the case of converted waves, the gathers can appear horizontal even though the velocity may be wrong (Menyoli, 2002).

In conclusion, velocity model building with converted waves is much more elaborate than in the monotypic case. Although the effort could be reduced by processing SS data instead of PS, the resulting simplifications would be compensated with the problems arising during the acquisition.

One technique for the determination of P velocities was recently introduced by Duveneck (2004). It evaluates wave field attributes obtained from a common reflection surface (CRS) stack of PP data in a tomographic procedure. We suggest to extend the method such that we combine the wave field attributes for PP and PS data in order to simulate SS wave field attributes.

After a brief summary of the CRS stack and NIP wave tomography, we introduce our method. Due to the already mentioned properties of converted waves the combination of PP and PS parameters is not straightforward. We will explain the specific problems in more detail and, following that section, present solutions.

ZERO OFFSET CRS AND NIP WAVE TOMOGRAPHY

The CRS stacking technique was introduced by Mueller (1999) to obtain a simulated zero offset section. The CRS stack can be considered as an extension of the classic CMP method, where stacking is carried out over offsets, while in the CRS technique the stack is applied over offsets and midpoints. This leads to a much larger number of contributing traces, and, thus, to a higher level of the signal to noise ratio.

Whereas the CMP operator is a hyperbola, the corresponding CRS operator is a surface of second order that includes the CMP operator as subset. Written in midpoint (x_m) and half-offset (h) coordinates, the CRS operator in the two-dimensional zero offset case reads,

$$T_{ZO}^2(\triangle x_m, \triangle h) = \left[T_0 + \frac{2 \sin \beta_0}{V_0} \triangle x_m \right]^2 + \frac{2\, T_0\, \cos^2 \beta_0}{V_0} \left[K_N\, \triangle x_m^2 + K_{NIP}\, \triangle h^2 \right] \quad . \qquad (1)$$

It contains three wave field attributes or parameters, namely, the incidence or emergence angle β_0; the curvature K_{NIP} of a wave generated by a point source at the normal incidence point (NIP), the so-called NIP wave; and the curvature K_N of a wavefront generated by an exploding reflector element, the so-called normal wave. Furthermore, the velocity V_0 is that at the source and receiver. The meaning of the attributes is also illustrated in Figure 1. The extension to 3D is straightforward (Müller, 2007).

The parameters are useful for a variety of applications (see, e.g. Mann, 2002) like attribute-based time migration, determination of geometrical spreading, migration weights, Fresnel zones, and multiple sup-

pression.

The application we will focus on in this work is the NIP wave tomography suggested by Duveneck (2004). According to that work, 'in a correct model, all considered NIP waves when propagated back into the Earth along the normal ray focus at zero traveltime'. The concept of focusing NIP waves was already introduced by Hubral and Krey (1980), and cast into a tomographic inversion by Duveneck (2004).

With the traveltime, emergence angle, and NIP wave curvature given by the CRS stack, dynamic ray tracing is performed in an initial model. Subsequent evaluation of the resulting NIP wave radius leads to an update of the velocity model, which then serves as input for the next iteration step. The procedure is repeated until convergence is achieved.

OFFSET CRS FORMULATION AND RAY BRANCH DECOMPOSITION

The physical interpretation of the attributes, e.g. K_{NIP}, which is evaluated in the NIP wave tomography is based on a one-way process. This is possible for monotypic waves because the up- and down-going ray paths coincide in the zero offset case. This assumption is not valid if converted waves are considered. In consequence, the corresponding expression for the CRS operator has five parameters now instead of three for the monotypic zero offset case. Since it is formally identical with the common offset CRS formulation, we will use this general form from now on.

In source (s) and receiver (g) coordinates, the common offset CRS formula reads,

$$T^2(s', g') = (T_0 + q \, \Delta g - p \, \Delta s)^2 + T_0 \left(G \, \Delta g^2 - S \, \Delta s^2 - 2 \, N \, \Delta s \, \Delta g \right) \quad, \tag{2}$$

where the first-order derivatives,

$$p = -\frac{\partial T}{\partial s} \quad, \text{ and } \qquad q = \frac{\partial T}{\partial g} \quad, \tag{3}$$

are the horizontal slownesses at the source and receiver, respectively. The second-order derivatives are given by

$$S = -\frac{\partial^2 T}{\partial s^2} \quad, \quad G = \frac{\partial^2 T}{\partial g^2} \quad, \text{ and } \qquad N = -\frac{\partial^2 T}{\partial s \, \partial g} \quad. \tag{4}$$

In three dimensions, the first-order derivatives are vectors and the second-order derivatives are matrices (see Vanelle, 2002).

Equation (2) is equal to the common offset CRS expression given by Bergler et al. (2002) (their equation (1)). The first- and second-order derivatives can also be expressed by incidence and emergence angles β_G and β_S, and the velocities V_S and V_G, where the indices S and G denote source and receiver; and the scalar elements A, B, C, D of the surface-to-surface propagator matrix introduced by Bortfeld (1989). The relations between these parameters are,

$$A = -\frac{S}{N} \quad, \quad B = \frac{1}{N} \quad, \quad C = -N - \frac{SG}{N} \quad, \text{ and } \qquad D = \frac{G}{N} \quad, \tag{5}$$

and

$$p = \frac{\sin \beta_S}{V_S} \quad, \qquad q = \frac{\sin \beta_G}{V_G} \quad, \tag{6}$$

or,

$$S = -\frac{A}{B} \quad, \qquad G = \frac{D}{B} \quad, \qquad N = \frac{1}{B} \quad, \tag{7}$$

and

$$\sin \beta_S = p \, V_S \quad, \qquad \sin \beta_G = q \, V_G \quad, \tag{8}$$

respectively.

For zero offset and monotypic waves, it follows from the symmetry that $p = -q$ and $G = -S$. With $g = x_m + h, s = x_m - h$, equation (2) reduces to (1) in that case, and the zero offset attributes can be expressed by

$$q = -p = \frac{\sin \beta_0}{V_0} \quad, \qquad G = -S = \frac{\cos^2 \beta_0}{2 \, V_0} \left(K_{NIP} + K_N \right) \quad, \qquad N = \frac{\cos^2 \beta_0}{2 \, V_0} \left(K_{NIP} - K_N \right) \quad, \tag{9}$$

or

$$\sin \beta_0 = q\, V_0 \quad , \qquad K_N = \frac{V_0}{\cos^2 \beta_0}(G - N) \quad , \qquad K_{NIP} = \frac{V_0}{\cos^2 \beta_0}(G + N) \quad , \qquad (10)$$

respectively.

Since there is no equivalent one-way process in the case of converted waves, we have to consider the individual ray segments in order to find a way of combining the PP and PS wave field attributes. In the following, we will use a parabolic variant of (2). It is valid for the traveltime of a reflected or converted event as well as for each of the individual segments if a reflection point with the coordinate r is introduced.

A PP zero offset event consists of two identical P segments from s to r (or from r to g). Let S_{PP}, G_{PP}, N_{PP} denote the parameters of the reflected, i.e. PP, event, and $S_P \ne G_P$, N_P those of the single P segment, i.e., the traveltime of the reflected event can be expressed by

$$
\begin{aligned}
T_{PP}(s', g') &= T_{0-PP} + q_{PP}\,\Delta g - p_{PP}\,\Delta s + \frac{1}{2}\left(G_{PP}\,\Delta g^2 - S_{PP}\,\Delta s^2 - 2\,N_{PP}\,\Delta s\,\Delta g\right)\\
&= 2\left(T_{0\,P} + q_P^r\,\Delta r - p_P\,\Delta s\right) + G_P\,\Delta r^2 - S_P\,\Delta s^2 - 2\,N_P\,\Delta s\,\Delta r\\
&= 2\,T_P(s', r') \quad ,
\end{aligned}
\tag{11}
$$

where q_P^r is the slowness at the reflector. In (11), $q_{PP} = -p_{PP}$ and $G_{PP} = -S_{PP}$ due to the symmetry.

Similarly, a zero offset SS event with parameters S_{SS}, G_{SS}, N_{SS} has two identical individual S segments with $S_S \ne G_S$, N_S:

$$
\begin{aligned}
T_{SS}(s', g') &= T_{0-SS} + q_{SS}\,\Delta g - p_{SS}\,\Delta s + \frac{1}{2}\left(G_{SS}\,\Delta g^2 - S_{SS}\,\Delta s^2 - 2\,N_{SS}\,\Delta s\,\Delta g\right)\\
&= 2\left(T_{0\,S} + q_S\,\Delta g - p_S^r\,\Delta r\right) + G_S\,\Delta g^2 - S_S\,\Delta r^2 - 2\,N_S\,\Delta r\,\Delta g\\
&= 2\,T_S(r', g') \quad ,
\end{aligned}
\tag{12}
$$

where p_S^r is the slowness at the reflector. In (12), $q_{SS} = -p_{SS}$ and $G_{SS} = -S_{SS}$ due to the symmetry.

Finally, a zero offset PS event described by S_{PS}, G_{PS}, N_{PS} consists of two individual different segments, the P and S segments, with S_P, G_P, N_P and S_S, G_S, N_S, respectively:

$$
\begin{aligned}
T_{PS}(s', g') &= T_{0-PS} + q_{PS}\,\Delta g - p_{PS}\,\Delta s + \frac{1}{2}\left(G_{PS}\,\Delta g^2 - S_{PS}\,\Delta s^2 - 2\,N_{PS}\,\Delta s\,\Delta g\right)\\
&= T_{0\,P} + q_P^r\,\Delta r - p_P\,\Delta s + \frac{1}{2}\left(G_P\,\Delta r^2 - S_P\,\Delta s^2 - 2\,N_P\,\Delta s\,\Delta r\right)\\
&\quad + T_{0\,S} + q_S\,\Delta g - p_S^r\,\Delta r + \frac{1}{2}\left(G_S\,\Delta g^2 - S_S\,\Delta r^2 - 2\,N_S\,\Delta r\,\Delta g\right)\\
&= T_P(s', r') + T_S(r', g')
\end{aligned}
\tag{13}
$$

Elimination of the reflector coordinate in Equations (11), (12), and (13) by evaluating Snell's law leads to relationships between the coefficients of the single and reflected rays. For the PP case, we find

$$p_{PP} = p_P = -q_{PP} \quad , \qquad S_{PP} = S_P + \frac{N_P^2}{2\,G_P} = -G_{PP} \quad , \qquad N_{PP} = \frac{N_P^2}{2\,G_P} \quad . \tag{14}$$

Correspondingly, for the SS case it follows that

$$q_{SS} = q_S = -p_{SS} \quad , \qquad S_{SS} = S_S + \frac{N_S^2}{2\,G_S} = -G_{SS} \quad , \qquad N_{SS} = \frac{N_S^2}{2\,G_S} \quad . \tag{15}$$

Finally, for the converted wave,

$$p_{PS} = p_P \quad , \qquad q_{PS} = q_S \quad ,$$

$$S_{PS} = S_P + \frac{N_P^2}{G_P + G_S} \quad , \qquad G_{PS} = -S_S - \frac{N_S^2}{G_P + G_S} \quad , \qquad N_{PS} = \frac{N_P\, N_S}{G_P + G_S} \quad . \tag{16}$$

(a) PP ray path   **(b)** SS ray path   **(c)** PS ray path
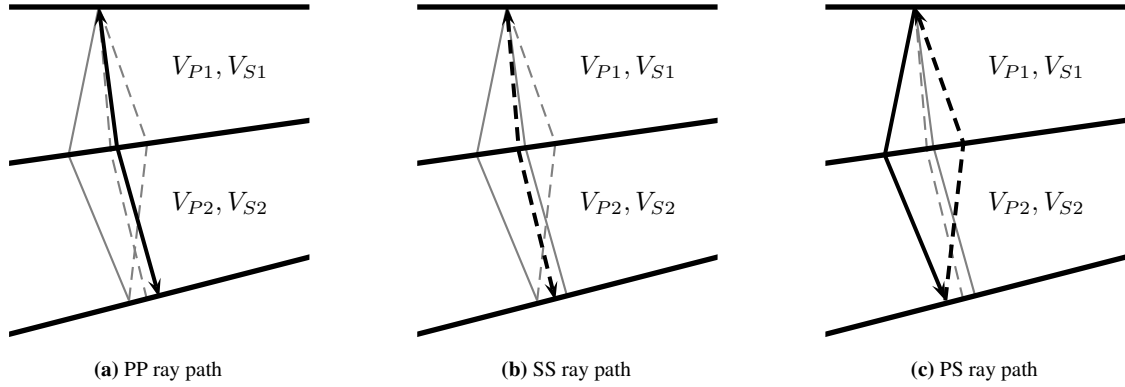
Figure 2: Zero-offset ray paths for (a) PP, (b) SS, and (c) PS reflections, where $V_{P1}/V_{S1} \neq V_{P2}/V_{S2}$. Solid lines indicate P-waves; dashed lines correspond to S-waves.

The same result can be obtained with the propagator formalism (Bortfeld, 1989). Combining Equations (9) and (15), we find that the NIP wave curvature corresponding to the zero-offset SS reflection is given by

$$K_{NIP-SS} = -\frac{V_{0\,S}}{\cos^2 \beta_{0\,S}} S_S \quad . \tag{17}$$

According to (15), the angle $\beta_{0\,S}$ is the incidence angle at the receiver for the PS case, i.e., $\sin \beta_{0\,S} = q_{PS}\, V_{S\,0}$. With (16), we can now express S_S in Equation (17) by

$$S_S = -G_{PS} - \frac{N_{PS}^2}{S_{PS} - S_P} \quad , \tag{18}$$

where S_P follows from Equations (9) and (14) as

$$S_P = -\frac{\cos^2 \beta_{0\,P}}{V_{0\,P}\, K_{NIP-PP}} \quad . \tag{19}$$

Equations (17) to (19) provide the NIP wave curvature of a simulated SS wave. To perform NIP wave tomography, we also require the emergence angle for the ray tracing, $\beta_{0\,S}$, which is given by q_{PS}, and the traveltime, which can be obtained from the difference between T_{PS} and $T_{PP}/2$.

In conclusion, by combining the parameters from the PP and PS zero-offset CRS stacks, we can now, in theory, apply NIP wave tomography to obtain the shear velocity model. In practice, however, the determination of K_{NIP-SS} is not as straight-forward as described here. We discuss the reasons and other practical issues in the following section.

PRACTICAL CONSIDERATIONS

For the derivation of the relationship between K_{NIP-SS} and the CRS parameters of the PP and PS data we have implicitly assumed that the ray paths for PP, PS, and SS coincide. Whereas in the monotypic case, the up- and down-going ray segments coincide and are normal to the reflector, this is not generally true for the zero offset converted wave, as demonstrated by Figure 2. The P and S ray path segments are only then identical when the ratio of P and S velocities remains constant throughout the medium. If that were the case, however, we could simply compute our shear velocity model by applying a scale factor to the P model.

To address this problem, we assume that the distance $\triangle r$ between the reflection point of the zero-offset PP reflection and the conversion point of the zero-offset PS reflection lies within a paraxial vicinity. In that case, $\triangle r$ can be expressed by

$$\triangle r = \frac{p_{PS} - p_{PP}}{N_P} \quad . \tag{20}$$

In (20), the one-way parameter N_P for the P wave is not directly available from the PP CRS parameters, but it can be easily computed with dynamic ray tracing (DRT). In fact, computing N_P does not even require an additional effort as DRT is performed within the NIP wave tomography. Considering the traveltime of the P wave to the conversion point, with

$$T_P^2(s, r') = \left(\frac{T_{0-PP}}{2} + q_P^r \, \triangle r \right)^2 + G_P \triangle r^2 \quad , \tag{21}$$

where q_P^r and G_P are also known from the DRT for the NIP wave tomography, we can now carry out DRT with the take-off angle corresponding to the PS wave and compute the value of S_P for this ray path to be combined with the PS parameters and obtain K_{NIP-SS}. Although this step requires additional DRT, the effort is negligible since only a single ray needs to be traced. Furthermore, the ray end point gives us a measure of the accuracy as it should coincide with $r' = r + \triangle r$, and therefore provides a means for quality control.

Combining parameters from PP and PS CRS stacks requires that the events under consideration need to be identified in both sections. The technique that springs to mind for solving this issue is slope matching, i.e., comparing the slowness vectors of the P segments of the PP and PS rays, p_{PP} and P_{PS}. However, as we have seen above, the ray paths do not coincide for media where the V_P/V_S ratio is not constant. In conclusion, the slownesses do not coincide either. In contrast to the 'PP+PS=SS' method (Grechka and Tsvankin, 2002), where slope matching in the pre-stack domain is performed to obtain SS traveltimes from combining PP and PS measurements, we are working in the post-stack domain, where their algorithm cannot be applied.

Although it is possible to manually identify key events in the sections and use these to assign weaker events, such a procedure would countermand one of the major advantages of NIP wave tomography, namely that user intervention, e.g., picking, is kept to a minimum. We recognise that this challenging step needs further investigation if it is intended to be carried out in a fully-automatic fashion.

There are additional issues related to the CRS stacking of converted waves that also occur in CCP stacking, like the polarity reversal of the shear wave or wave field separation prior to the stacking. Since the emphasis of this work is on the combination of the PP and PS parameters to obtain SS parameters, we refer the reader to the literature suggested in the introduction.

CONCLUSIONS

We have introduced a new method to obtain the NIP wave curvature of an SS reflection from CRS stacking of PP and PS data. Knowledge of the NIP wave curvature allows to perform NIP wave tomography for shear waves. Since the necessary parameters are available from the PP and PS sections, the shear model can now be determined without acquiring SS data.

As soon as the V_P/V_S ratio is not constant throughout the medium, an additional ray tracing step is required to account for the difference in the PP and PS emergence angles. Since only single rays need to be traced in the P model, this step does not degrade the numerical efficiency. Furthermore, dynamic ray tracing is already embedded in the NIP wave tomography.

ACKNOWLEDGEMENTS

REFERENCES

Al-Yahya, K. M. (1989). Velocity analysis by iterative profile migration. *Geophysics*, 54:718–729.

Bergler, S., Duveneck, E., Hoecht, G., Zhang, Y., and Hubral, P. (2002). Common-reflection-surface stack for converted waves. *Studia geophysica et geodetica*, 46:165–175.